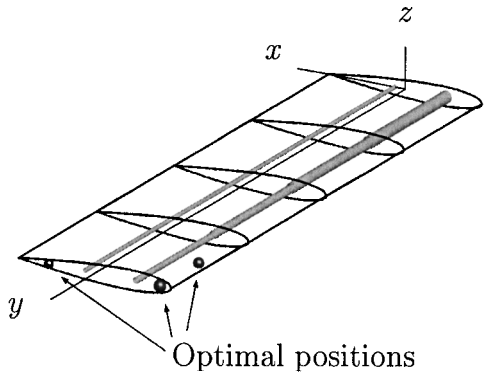

Fig. 2 Optimal design.

design. The maximum feasible mass, 1 kg, is located at the wing-tip leading-edge position, 0.70 kg at the inner leading-edge position, and 0.49 kg at the wing-tip trailing-edge position.

Both the flutter stability and frequency constraints in Eqs. (9) and (10) are active for the optimal design, meaning that both the target flutter speed and frequency are reached. At the flutter speed, a first torsion/first bending type of flutter occurs, whereas the other modes show a significantly higher damping for the considered speed range. The divergence speed for the optimal design is $u_D = 84$ m/s (274 ft/s). This is higher than the minimum feasible value $\hat{u}_D = 61$ m/s (200 ft/s), and the static stability constraint Eq. (11) is not active. However, the static stress at the root of the front spar is the maximum feasible, and the constraint in Eq. (12) representing this location is active. To summarize, a feasible design has been obtained.

Conclusions

The optimization formulation of minimizing structural weight was successfully applied to the present aeroelastic design problem, and a feasible design was obtained using numerical optimization. However, the design process was not without flaws. Whereas the low torsional stiffness of the two-spar design enabled a low flutter speed and frequency, the wing was also very prone to divergence. Taking wing sweep into account revealed that no significant improvement was to be expected for moderate sweep. Instead, the optimization resolved this obstacle by tapering the front spar only, which increased the divergence speed through bending/torsion coupling.

Another interesting feature of the optimal design is that the mass balancing tends to inertially decouple the two first modes of vibration of the unbalanced configuration. Without mass balancing, the first two modes of vibration are strongly influenced by both bending and torsion, mainly due to the coupling introduced by the tapered front spar. With mass balancing, the wing displays almost decoupled first bending and torsion modes.

Also note that the influence of the microflaps has not been taken into account in this study, and it is recommended that the analysis be extended to include a representative model of the actuators. The main conclusion is that the two-spar concept may be an option for the structural design of the wind-tunnel model. However, care must be taken with respect to the approximations made, and the model is fairly complex to realize. Other possible concepts, such as a plate design, may be more tractable. Of course, the present optimization-based approach to aeroelastic design may be useful in future studies as well.

Acknowledgments

The first author was financially supported by the Swedish Research Council for Engineering Sciences, and this work was performed while the first author was a visiting scientist at Stanford University. Mikael Holden is gratefully acknowledged for suggesting the investigation of the two-spar design, Stefan Bieniawski for providing material properties, and Hak-Tae Lee for computing the airfoil properties.

References

[1]Kroo, I., "Aerodynamic Concepts for Future Aircraft," AIAA Paper 99-3524, June 1999.

[2]Bisplinghoff, R. L., Ashley, H., and Halfman, R. L., *Aeroelasticity*, Dover, New York, 1996, pp. 695–712, 724–735, and 251–281.

[3]French, M., and Eastep, F. E., "Aeroelastic Model Design Using Parameter Identification," *Journal of Aircraft*, Vol. 33, No. 1, 1996, pp. 198–202.

[4]Dowell, E. H., Curtiss, H. C., Scanlan, R. H., and Sisto, F., *A Modern Course in Aeroelasticity*, Kluwer, Dordrecht, The Netherlands, 1989, pp. 129–157.

[5]Borglund, D., and Kroo, I. M., "Aeroelastic Design Optimization of the Micro Trailing Edge Flap Flexible Wing," *Proceedings of the CEAS/AIAA/AIAE International Forum on Aeroelasticity and Structural Dynamics*, Madrid, Spain, Vol. 2, 2001, pp. 487–495.

[6]Bäck, P., and Ringertz, U. T., "On the Convergence of Methods for Nonlinear Eigenvalue Problems," *AIAA Journal*, Vol. 35, No. 6, 1997, pp. 1084–1087.

[7]Svanberg, K., "The Method of Moving Asymptotes (MMA) with some Extensions," *Optimization of Large Structural Systems*, edited by G. I. N. Rozvany, Vol. 1, Kluwer, Dordrecht, The Netherlands, 1993, pp. 555–566.

[8]Haftka, R. T., and Adelman, H. M., "Sensitivity of Discrete Systems," *Optimization of Large Structural Systems*, edited by G. I. N. Rozvany, Vol. 1, Kluwer, Dordrecht, The Netherlands, 1993, pp. 289–311.

[9]Ringertz, U. T., "On Structural Optimization with Aeroelasticity Constraints," *Structural Optimization*, Vol. 8, No. 1, 1994, pp. 16–23.

[10]Seyranian, A. P., "Sensitivity Analysis of Multiple Eigenvalues," *Mechanics of Structures and Machines*, Vol. 21, No. 2, 1993, pp. 261–284.

Speed-Sensitivity Analysis by a Genetic Multiobjective Optimization Technique

Luciano Blasi,* Luigi Iuspa,† and Giuseppe Del Core‡
Second University of Naples, 81031 Aversa, Italy

Introduction

THE availability of effective tools that quickly provide aircraft overall characteristics sensitivity for different figures of merit is a very important factor during the early phase of the design process (that is, conceptual design phase). Typical figures of merit used are the following ones: gross weight, empty weight, fuel burned, and cruise speed. A multiobjective optimization technique can be used to understand how optimum configurations change as different objectives are selected. An example of such a parametric multiobjective approach can be found in Ref. 1. In this mentioned work a global figure of merit is defined as a weighted sum of selected objective functions. An effective gradient-based optimization technique[2,3] is used, and different design solutions are obtained by changing the weight value. This Note deals with the application of a genetic multiobjective optimization technique in the field of aircraft requirements analysis. This procedure takes advantage of the well-known genetic parallel-like searching method and allows us to obtain sensitivity curves by only one optimization run. Once a specific requirement has been selected (for example, range, speed, ceiling, takeoff distance, etc.), these curves provide a deeper understanding of the requirement effect on the aircraft configuration. In particular, cruise speed effect has been evaluated in this Note. Such a type of procedure can thus be proposed as a very useful and effective tool for tradeoff studies aimed at the final freeze of requirements. Classical

Received 1 December 2001; revision received 20 June 2002; accepted for publication 1 July 2002.

*Senior Research Scientist, Department of Aerospace Engineering, Via Roma 29.

†Research Scientist, Department of Aerospace Engineering, Via Roma 29.

‡Associate Professor, Department of Aerospace Engineering, Via Roma 29. Member AIAA.

Pareto concept[4] has been used to define the optimum solution (that is, a solution is called Pareto optimal, or nondominated, if it is not possible to improve any objective functions without deteriorating at least one of the others). As will be shown in the following section, the concept of nondominated solution can be easily used to define a fitness function driving all of the optimization process. Detailed examples of genetic multiobjective optimization procedures, related to aerodynamic as well as structural design, can be found in the literature.[5–9]

Problem Definition

Multiobjective optimization technique is well suited to answer one of the questions that is typically raised during the requirements analysis concerning optimum cruise speed identification, that is, if it is better to favor a faster configuration (higher utilization) or a lower one (less weight). Therefore, maximum takeoff weight and cruise speed have been selected as the two objectives to be optimized. Such a type of selection provides the designer with all of the information concerning the configuration evolution (from the lowest to the fastest one) allowing the reduction of uncertainties about proposed speed requirement. As an example, the procedure has been applied to the preliminary definition of a short medium-range transport aircraft configuration powered by turbofan engines. Design variables and constraint functions selected have been summarized in Tables 1–3. They are based mainly on Ref. 10; however, the ranges of some design variables (wing sweep, wing taper ratio, engine thrust scaling factor) have been extended to verify procedure capability to explore a wider design domain. For the same reason low-speed requirements have been slightly relaxed in order to be consistent with a thrust level range as wide as possible. Compared to Ref. 10, no other changes have been made as for the other mission requirements. Starting from a basic population of 300 individuals, 150 couples have been selected and mated to generate 300 new offspring. To keep a constant

Table 1 Design variables

Variable, units	Range/values	String length, bits
Wing sweep, deg.	5–35	6
Wing t/c change	0–0.05	6
Wing area, m^2	80–130	7
Takeoff flap deflection, deg	0, 10, 15, 20	6
Landing flap deflection, deg	25, 30, 35, 40	6
Wing taper ratio	0.15–0.50	6
Wing aspect ratio	7–9.5	6
Configuration index	1, 2, 3, 4	6
Engine thrust scaling factor (T/T_{ref})	1.0–1.5	6
Cruise altitude, m × 1000	8.8, 9.1, 9.4, 9.8, 10.1, 10.4, 10.7, 11.0	6

Table 2 Configuration index value vs aircraft configuration

Configuration index	Aircraft configuration
1	5 abreast, fuselage-mounted engines
2	6 abreast, fuselage-mounted engines
3	5 abreast, wing-mounted engines
4	6 abreast, wing-mounted engines

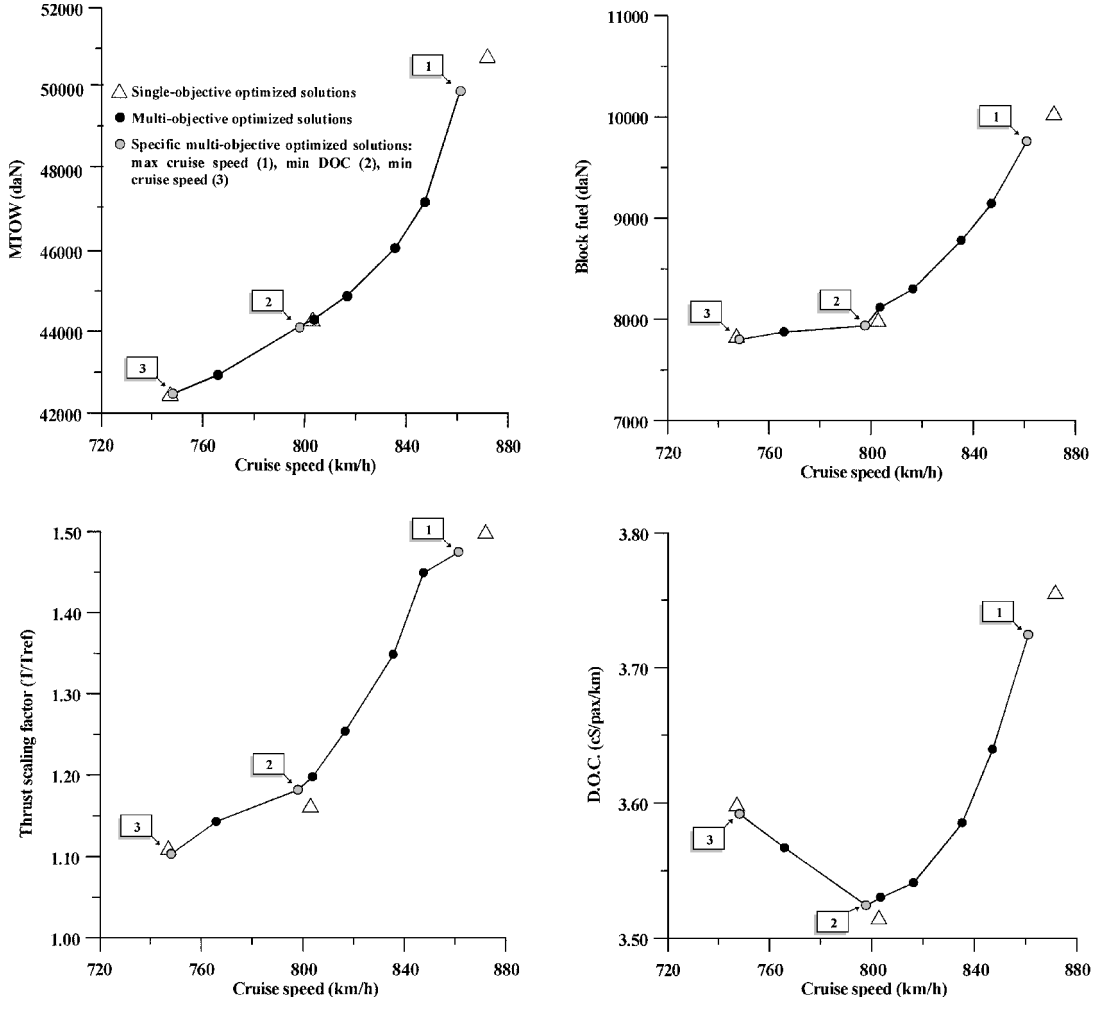

Fig. 1 Examples of sensitivity curves: MTOW, block fuel, thrust scaling factor, and DOC vs cruise speed. Comparison of specific Pareto optimal solutions, that is, max cruise speed (1), min DOC (2), and min cruise speed (3) configurations, with the similar ones provided by a single-objective optimization procedure (white △).

Table 3 Constraint functions parameters

Constraint function, units	Min	Max	Exp
Rate of climb at cruise altitude, m/s	1.50	50	2
Balanced field length, m	0	1830	2
Landing field length, m	0	1525	2
Approach speed, km/h	0	240	2
Cruise range/design range	0.5	1.0	2
Second segment climb gradient	0.024	0.30	2
Mission fuel/max fuel capacity	0	1.0	2
Wing tip chord, m	1.0	4.0	2

Table 4 Genetic optimization parameters

Parameter	Value/type
Crossover	Single-cut
Bitwise mutation rate	0.04
Couples selection criteria	Roulette-wheel (up to 40th generation) + random-walk
Fitness sharing	Linear

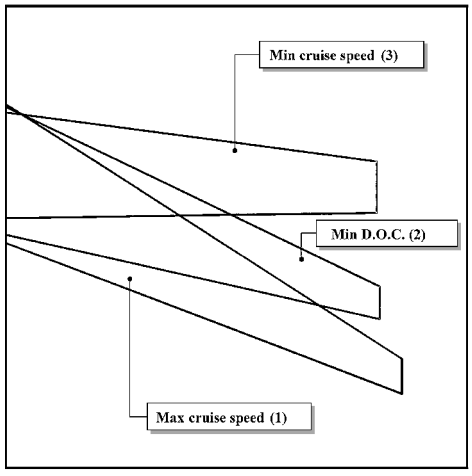

Fig. 2 Right-half-wing planform evolution along Pareto curve. Comparison of solutions 1, 2, and 3 wing planform.

population size during evolution, the resulting extended population (parents + offspring) has been sorted and trimmed by discarding the worst individuals. By using a Pareto-ranking criteria,[11] the fitness function of individual i at generation n has been defined in the following manner:

$$fit_i^{(n)} = N_{\text{ind}} - rank_i^{(n)} \tag{1}$$

where N_{ind} is the population size. Moreover, a linear fitness-sharing technique[11] has been adopted to improve solutions distribution along the Pareto front. Once the 100th generation has been analyzed, the optimization process is automatically stopped. This number of generations is sufficient to allow a satisfactory definition of the Pareto curve. Table 4 summarizes the selected genetic optimization parameters. As can be noticed, roulette-wheel criteria has been used up to the 40th generation; it was observed that the population average fitness quickly reached a rather high value, and so for the remaining generations a random-walk criteria has been preferred and used.

Results

Examples of speed-sensitivity curves are shown in Fig. 1. In particular, maximum takeoff weight (MTOW), block fuel, thrust scaling factor, and direct operating cost (DOC) sensitivity curves have been reported. As can be noticed, minimum DOC optimum cruise speed (around 800 km/h) has been well identified. To verify multiobjective optimizer effectiveness in sampling design domain and final solutions reliability as well, a comparison with solutions provided by the single-objective procedure already mentioned[10] has been made. As shown in Fig. 1, three specific solutions, that is, max

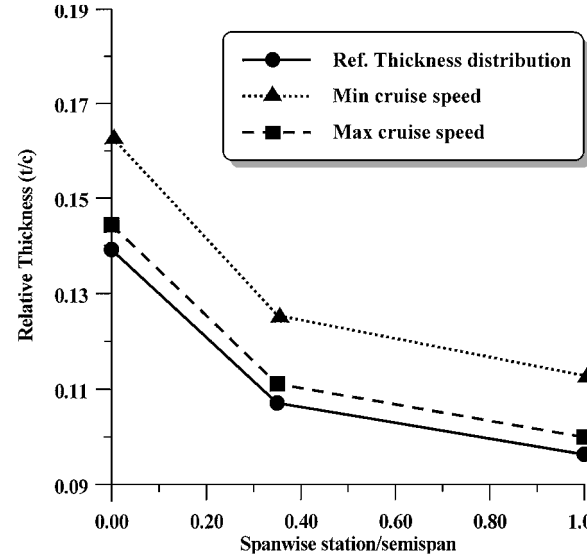

Fig. 3 Wing thickness distribution comparison.

cruise speed (solution number 1), min DOC (solution number 2), min cruise speed (solution number 3), have been highlighted with gray circles and compared to the similar ones (white triangles) provided by the single-objective procedure. Although the single-objective procedure has been able to define a slightly faster (and heavier) configuration, results provided by the multiobjective optimizer appear to lie on the same trend lines in all of the cases. Examples of configuration evolution, from the fastest to the lowest one, are shown in Figs. 2 and 3. The former shows right-half-wing superposition of solution numbers 1, 2, and 3. The latter shows solutions 1 and 3 wing thickness distribution compared to the reference one. Solutions 2 thickness distribution has not been reported being very close to the solution 1 thickness distribution.

Conclusions

A genetic multiobjective optimization technique, based on the Pareto curve concept, has been developed. This procedure has been applied for the requirements analysis of a short medium-range transport aircraft. In particular, cruise speed effect has been analyzed. Final results have shown the multiobjective optimization procedure capability to provide useful sensitivity curves of the overall aircraft characteristics for the selected requirement. These curves, providing all of the information on the configuration evolution, allow the designer to have a deeper understanding of the proposed speed requirement. Comparison with single-objective-genetic-optimized solutions (max cruise speed, min DOC, min cruise speed) has confirmed the multiobjective procedure effectiveness in sampling design domain and final solutions reliability as well. Such a type of procedure can thus be proposed as a very effective tool for trade-off studies aimed at the final definition of aircraft requirements in the early stage of the design process.

References

[1]Malone, B., and Mason, W. H., "Aircraft Concept Optimization Using Parametric Multiobjective Figures of Merit," *Journal of Aircraft*, Vol. 33, No. 2, 1996, pp. 444, 445.

[2]Malone, B., and Mason, W. H., "Multidisciplinary Optimization in Aircraft Design Using Analytic Technology Models," *Journal of Aircraft*, Vol. 32, No. 2, 1995, pp. 431–438.

[3]Sobieszczanski-Sobieski, J., "Sensitivity Analysis and Multidisciplinary Optimization for Aircraft Design: Recent Advances and Results," *Journal of Aircraft*, Vol. 27, No. 12, 1990, pp. 993–1001.

[4]Rao, S. S., "Further Topics in Optimization," *Engineering Optimization: Theory and Practice*, 3rd ed., Wiley, New York, 1996, pp. 779–783.

[5]Coello, C. A., and Christiansen, A. D., "Multiobjective Optimization of Trusses Using Genetic Algorithms," *Computer and Structures*, Vol. 75, No. 6, 2000, pp. 647–660.

[6]Crossley, W. A., Cook, A. M., Fanjoy, D. W., "Using the Two-Branch Tournament Genetic Algorithm for Multiobjective Design," *AIAA Journal*, Vol. 37, No. 2, 1999, pp. 261–267.

[7]Vicini, A., and Quagliarella, D., "Inverse and Direct Airfoil Design Using a Multiobjective Genetic Algorithm," *AIAA Journal*, Vol. 35, No. 9, 1997, pp. 1499–1505.

[8]Jones, B. R., Crossley, W. A., and Lyrintzis, A., "Aerodynamic and Aeroacustic Optimization of Rotorcraft Airfoils via a Parallel Genetic Algorithm," *Journal of Aircraft*, Vol. 37, No. 6, 2000, pp. 1088–1096.

[9]Obayashi, S., Yamaguchi, Y., and Nakamura, T., "Multiobjective Genetic Algorithm for Multidisciplinary Design of Transonic Wing Planform," *Journal of Aircraft*, Vol. 34, No. 5, 1997, pp. 690–693.

[10]Blasi, L., Iuspa, L., and Del Core, G., "Conceptual Aircraft Design Based on a Multiconstraint Genetic Optimizer," *Journal of Aircraft*, Vol. 37, No. 2, 2000, pp. 350–354.

[11]Obayashi, S., "Pareto Genetic Algorithm for Aerodynamic Design Using the Navier–Stokes Equation," *Genetic Algorithms in Engineering and Computer Science*, Wiley, New York, 1997, pp. 245–266.

Flow Past an Airfoil with a Leading-Edge Rotation Cylinder

X. Du* and T. Lee†
McGill University, Montreal, Quebec H3A 2K6, Canada
F. Mokhtarian** and F. Kafyeke††
Bombardier Aerospace, Dorval, Quebec H4S 1Y9, Canada

Introduction

THE delay of boundary-layer separation and the enhancement of the lift-to-drag ratio of an airfoil are always of great importance, not only to the design of advanced aircraft, but also to the control of the boundary-layer flow. Experimental control schemes, such as suction, blowing, vortex generators, turbulence augmentation, and the use of a moving wall[1–13] have been employed with varied degrees of success. By use of an airfoil with upper surface formed by a belt moving over two rollers, Favre[1] successfully delayed the boundary-layer separation up to an angle of attack α of 58 deg and obtained a maximum lift coefficient $C_{l\,\max}$ of 3.5. Steele and Harding[3] studied the use of rotating cylinders to improve ship maneuverability, using flow visualization and force measurements. Tennant et al.[4] conducted tests with a wedge-shaped flap having a rotating cylinder as the leading edge. Tennant et al.[5] also tested the circulation control for a symmetrical airfoil with a rotating cylinder at the trailing edge and reported that, at a zero angle of attack, a coefficient of lift of 1.2 was obtained for a normalized cylinder rotation, Ω (equal to u_s/u_∞, where u_s is the cylinder surface speed and u_∞ is the freestream velocity) of 1.2. It is now clear that moving-surface boundary-layer control involves the reduction of the initial boundary-layer growth by minimizing the relative velocity between the cylinder surface and the freestream and that, through the retardation of the initial boundary-layer growth and the subsequent delay of the separation of the boundary layer, increases in circulation and lift can then be achieved. Recently, Modi et al.[10] investigated the potential of application of a rotating cylinder at the leading edge of the airfoil of high-lift standard takeoff and landing-type aircraft. The effectiveness of moving-surface boundary-layer control on a symmetrical Joukowsky airfoil has been studied at length[6–12] through surface pressure measurement and flow visualization methods, as well as a six-axis force balance. An excellent review on the moving-surface boundary-layer control is given by Modi.[12]

In summary, the potential of a leading-edge rotating cylinder (LERC) as a boundary-layer control device has been investigated by researchers elsewhere; however, most of the work has focused primarily on exploratory studies or force measurements. No quantitative information of the effects of the cylinder rotation on the fluid dynamics process, especially the behavior of the boundary layer and the wake structure, was documented. The main objective of this study was to measure and characterize the effects of a LERC on the growth, development, and separation of the boundary layers and wake structures developed on and behind a symmetric airfoil by using hot-wire anemometry and smoke-flow visualization methods. Surface pressure measurements were also made to quantify the variation of lift-to-drag ratio under the influence of cylinder rotation. The present measurements provide typical data for computer model validation.

Experimental Apparatus and Methods

The experiments were conducted in a $0.9 \times 1.2 \times 2.7$ m suction-type wind tunnel. The freestream turbulence intensity was 0.04% at $u_\infty = 30$ m/s. A NACA 0015 airfoil with a chord length c of 25.4 cm and a span of 38 cm, fabricated from a solid aluminum, was used as the test model. The airfoil was fitted with endplates to ensure a two-dimensional flow around the airfoil. The leading-edge region of the airfoil was specially designed to accommodate the LERC of a diameter $d = 0.1\,c$ and a length of 38 cm, as well as the base airfoil, that is, airfoil with no leading-edge modification, Fig. 1. The selection of the rather large cylinder diameter in comparison to the leading-edge radius ($r = 0.0248c$) of the base airfoil was based on the consideration of achieving a value of Ω as high as possible. The gap between the rotating cylinder and the main airfoil was set at 1.2 mm. The selection of the present gap size was based on the guidelines suggested by Tennant et al.[5] They reported that a gap size less than 3 mm wide is required to minimize any possible negative effects induced by the

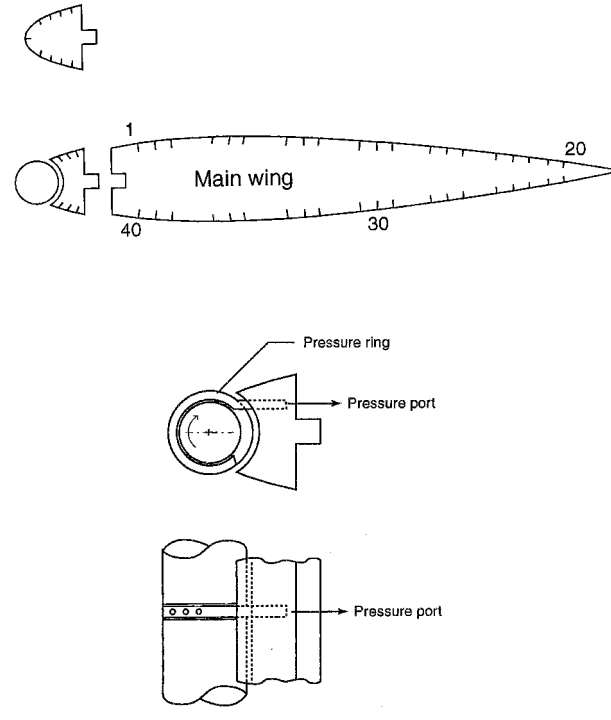

Fig. 1 Schematics of NACA 0015 airfoil model and the details of the pressure taps.

Received 24 January 2002; revision received 15 June 2002; accepted for publication 7 July 2002.

*Graduate Research Assistant, Aerodynamics Laboratory, Department of Mechanical Engineering.

†Associate Professor, Aerodynamics Laboratory, Department of Mechanical Engineering. Member AIAA.

**Section Chief, Advanced Aerodynamics. Member AIAA.

††Manager, Advanced Aerodynamics. Member AIAA.